Table IX. Mössbauer Parameters for Cis-Octahedral Inorganic Tin(IV) Compounds Containing Urea-Type Derivatives at 78 K

	$S^{a,b}$	$\Delta E_Q{}^a$
$SnCl_4 \cdot 2deu$	0.43	0.36
$SnCl_4 \cdot 2tmu$	0.41	0.83
$SnBr_4 \cdot 2dmu$	0.69	0.83
$SnBr_4 \cdot 2tmu$	0.77	0.80
$SnCl_4 \cdot 2detu$ [c]	0.31	0.0
$SnBr_4 \cdot 2dmtu$ [c]	0.40	0.0
$SnBr_4 \cdot 2detu$ [c]	0.39	0.0

[a] In mm/s; ±0.04 mm/s. [b] Relative to SnO_2. [c] From ref 1.

deviations from the octahedral symmetry[1] in the inorganic compounds, which would suggest a substantial electric quadrupole splitting. An explanation of this finding maybe that the p electron population in the p_x, p_y, and p_z orbitals of the inorganic tin(IV) series is altogether very small since the orbitals are filled only by covalent effects. This implies a larger s character in tin bonding orbitals and hence shorter Sn–L bonds and larger deviations from the octahedral symmetry for the cis-octahedral inorganic tin sites of Table IX with respect to the trans-octahedral compounds 1–8 of Table VIII. The first implication is consistent with the lower s electron density at the tin nucleus observed for the inorganic compounds of Table IX in comparison with the organotin compounds of Table VIII. The comparison of bond angles shows that the tin site in $SnCl_4 \cdot 2detu$,[1] for example, is more distorted than that in $Me_2SnCl_2 \cdot 2dmtu$ (Table V). The comparison of the bond lengths for $SnCl_4 \cdot 2detu$ (Sn–S = 2.49 and 2.52 Å; Sn–Cl = 2.48, 2.51, 2.55, and 2.58 Å)[1] shows that they are shorter than the corresponding ones in $Me_2SnCl_2 \cdot 2dmtu$ (Sn–S = 2.729; Sn–Cl = 2.616 Å).

This possible explanation of Mössbauer and crystallographic data based on a lack of the directional character of the p orbitals for the cis-octahedral tin(IV) compounds of Table IX needs, however, further data to be verified and substantiated.

Acknowledgment. Partial financial support by NATO RG 157.80 and by Ministero della Pubblica Istruzione, Rome, is acknowledged. We thank V. Corrado, A. Berton, and G. Silvestri for assistance.

Registry No. 1, 90457-51-5; 2, 90457-52-6; 3, 90457-56-0; $Me_2SnCl_2 \cdot 2urea$, 90457-50-4; $Me_2SnCl_2 \cdot 2dmu$, 36350-67-1; $Me_2SnCl_2 \cdot 2detu$, 90388-85-5; $Ph_2SnCl_2 \cdot 2deu$, 90388-86-6; $Ph_2SnCl_2 \cdot 2detu$, 90388-87-7; $Ph_2SnCl_2 \cdot 2tmu$, 90457-53-7; $Me_2SnCl_2 \cdot tmu$, 66625-87-4; $Me_2SnCl_2 \cdot tmtu$, 90457-54-8; $Ph_2SnCl_2 \cdot tmtu$, 90457-55-9; $SnCl_4 \cdot 2deu$, 82055-38-7; $SnCl_4 \cdot 2tmu$, 21470-10-0; $SnBr_4 \cdot 2dmu$, 90457-57-1; $SnBr_4 \cdot 2tmu$, 21470-11-1.

Supplementary Material Available: Table VII, giving the least-squares planes, and listings of the structure factor amplitudes with atomic thermal parameters for $Me_2SnCl_2 \cdot 2dmtu$, $Ph_2SnCl_2 \cdot 2dmtu$, and $Ph_3SnCl \cdot tmu$ (35 pages). Ordering information is given on any current masthead page.

(10) Greenwood, N. N.; Ruddick, J. N. R. *J. Chem. Soc. A* **1967**, *1679*.

Ligand Substitution Processes in Tetranuclear Carbonyl Clusters. 7. Molecular Structure and Carbon Monoxide Exchange Processes of $Co_4(CO)_9$(tripod), tripod = 1,1,1-Tris(diphenylphosphino)methane or $HC(PPh_2)_3$

Donald J. Darensbourg,* David J. Zalewski, and Terry Delord

Department of Chemistry, Texas A&M University, College Station, Texas 77843

Received March 27, 1984

A kinetic investigation of intermolecular carbon monoxide exchange reactions of $Co_4(CO)_9$(tripod) (tripod = 1,1,1-tris(diphenylphosphino)methane) with ^{13}C-labeled carbon monoxide is reported. The effect of incoming CO ligand concentration was examined by performing reactions under a pressure of carbon monoxide (up to 160 psi of ^{12}CO) employing $Co_4(^{13}CO)_9$(tripod) as substrate molecule. No dependence of the rate of CO incorporation into the tetranuclear cluster with carbon monoxide pressure was noted. Carbon monoxide substitutional parameters (rate constants and activation parameters) for CO displacement in the $Co_4(CO)_9$(tripod) species were found to be quite similar to those previously observed in the parent $Co_4(CO)_{12}$ and its monoligated phosphorus derivatives. These observations taken in toto imply a common mechanistic pathway for CO substitution in all these derivatives, i.e., a CO dissociative process. Reactions carried out utilizing phosphines and phosphites as incoming ligands were found to be complicated by ligand-dependent pathways for CO substitution. Phosphorus ligand substitution occurs stereoselectively at the apical cobalt sites. The crystal and molecular structure of $Co_4(CO)_9$(tripod) has been determined and is discussed in terms of the influence of structural factors on the reactivity of this species as well as in terms of the matching of the tripod ligand framework with the triangular face of the $Co_4(CO)_{12}$ moiety. The title compound forms monoclinic crystals in space group $I2/a$ with a = 21.943 (6) Å, b = 17.289 (7) Å, c = 26.137 (4) Å, β = 105.14 (2)°, V = 9585 (9) Å^3, and Z = 8. The discrepancy indices were R_1 = 0.052 and R_2 = 0.051 for 3001 reflections with $I > 3\sigma(I)$.

Introduction

Rate data for ligand substitution processes of low-valent mononuclear metal carbonyl derivatives are best interpreted in terms of mechanistic pathways identified with dissociative, interchange, or associative mechanisms (eq 1–3).[1,2] Although analogous substitution reactions in-

$$M(CO)_n \rightleftharpoons M(CO)_{n-1} + CO \xrightarrow{L} M(CO)_{n-1}L \text{ (D)} \quad (1)$$

0276-7333/84/2303-1210$01.50/0

$$M(CO)_n + L \rightleftharpoons M(CO)_n\cdots L \rightarrow M(CO)_{n-1}L + CO\ (I_d \text{ or } I_a) \quad (2)$$

$$M(CO)_n + L \rightleftharpoons M(CO)_nL \rightarrow M(CO)_{n-1}L + CO\ (A) \quad (3)$$

volving polynuclear metal carbonyl derivatives display similar kinetic behavior, alternative modes of reactivity can account for these data.[3] These additional considerations include cluster fragmentation and ligand-independent or ligand-dependent intramolecular metal–metal bond fission.[4]

Several researchers have employed $MnRe(CO)_{10}$ or a mixture of $Mn_2(CO)_{10}/Re_2(CO)_{10}$ to probe dimer disruption during both thermally and photochemically initiated ligand substitution reactions involving these group 7B species.[5] In analogous investigations Stolzenberg and Muetterties have utilized different isotopes of rhenium, i.e., $^{185}Re_2(CO)_{10}$ and $^{187}Re_2(CO)_{10}$, to address this question.[6] Thermal ligand substitution reactions were demonstrated to proceed via carbon monoxide dissociation from the intact dimer, whereas photochemical displacement of CO was shown, in part, to take place by a dimer disruption pathway.[7] Similar information is often available from isotopic studies involving the carbonyl ligands.[8] We have observed that reaction of a mixture of $Co_4(^{12}CO)_{12}$ and $Co_4(^{13}CO)_{12}$ with $P(OMe)_3$ yields only $Co_4(^{12}CO)_{11}P(OMe)_3$ and $Co_4(^{13}CO)_{11}P(OMe)_3$, hence indicative of ligand substitution without cluster fragmentation.[9]

In efforts to assess the importance of metal–metal bond fission during ligand substitution reactions involving tetranuclear cluster derivatives, where M–M bond cleavage does not necessarily lead to cluster fragmentation, we have determined rate parameters for carbon monoxide displacement in $Co_4(CO)_9$(tripod) (eq 4). This particular

$$Co_4(CO)_9(\text{tripod}) + n^{13}CO \rightleftharpoons Co_4(CO)_{9-n}(^{13}CO)_n(\text{tripod}) + n^{12}CO \quad (4)$$

species was chosen for examination because one triangular Co_3 face is rigidly held in place by the capping tridentate phosphine ligand, thereby greatly retarding metal–metal bond fission of at least three of the Co–Co bonds (see Scheme I where the opened circles indicate the unsaturated cobalt centers).[10] It is of course necessary to compare these rate data with those obtained in analogous

Scheme I

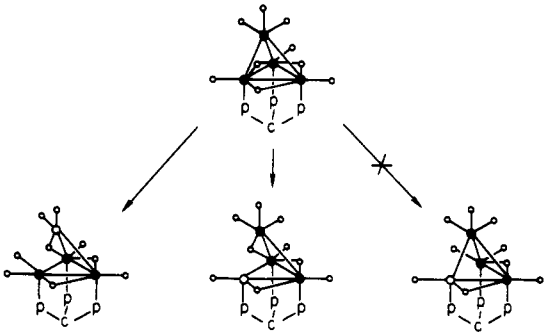

systems where this structural constraint is not present.[11-14] It is also of importance to accurately define the molecular structure of the ground-state molecule, specifically the metal–metal and metal–carbon bond distances. In this regard we report the X-ray structure determination of the $Co_4(CO)_9$(tripod) species.

Experimental Section

All manipulations were carried out either in an argon drybox or on a double manifold Schlenk vacuum line under an atmosphere of dry nitrogen. $Co_4(CO)_{12}$ was obtained from Strem Chemical, Inc., and was used without further purification. Solvents were dried by refluxing over sodium benzophenone ketyl under nitrogen. Carbon monoxide (93 atom % ^{13}CO) was obtained from Prochem, BOC Ltd., London.

Infrared spectra were recorded in 0.10–1.0-mm matched NaCl sealed cells on a Perkin-Elmer 283B spectrophotometer equipped with a Data Station and employing the PECDS software package provided by Perkin-Elmer or on an IBM FT-IR Model 85 spectrophotometer. Proton and ^{13}C NMR spectra were determined on a Varian EM390 and XL-200 spectrometer, respectively.

Preparations. 1,1,1-Tris(diphenylphosphino)methane (tripod), $HC(PPh_2)_3$, was prepared from $(Ph_2P)_2CH^-Li(TMEDA)^+$ and Ph_2PCl in tetrahydrofuran in 61% overall yield according to the method previously described.[15] [^1H NMR (CD_2Cl_2) 4.25 (CH, 1 H, s), 7.1–7.4 ppm (aromatic protons, 30 H, m).]

$Co_4(CO)_9$(tripod). This cluster derivative was prepared in a manner quite similar to that described by Osborn and co-workers.[15] A solution of tripod (1.04 g, 1.81 mmol, dissolved in 250 mL of methylcyclohexane with heating to 70 °C) was added dropwise under nitrogen to a refluxing $Co_4(CO)_{12}$ solution (0.873 g, 1.53 mmol, in 150 mL of hexane) over a 75-min time period. The refluxing was continued for an additional 75 min before the reaction mixture was allowed to cool at room temperature. The precipitate that formed upon cooling was isolated by removing the solution via a cannula. The product was washed twice with 50 mL of hexane, dissolved in methylene chloride, filtered, and isolated by evaporating the solvent under vacuum. A 1.36-g sample of $Co_4(CO)_9$(tripod) (1.29 mmol, 94.2% yield) was recovered. Purification of $Co_4(CO)_9$(tripod) was accomplished by using a silica gel column (60–200 mesh). The complex was eluted with a 50% mixture of CH_2Cl_2 and hexane under a nitrogen atmosphere. Crystals suitable for X-ray analysis were obtained from THF upon addition of hexane: IR (cm^{-1} in CH_2Cl_2) 2049 (s), 2000 (vs), 1972 (sh), 1778 (m), (cm^{-1} in THF) 2045 (s), 1997 (vs), 1970 (sh), 1784 (s), (cm^{-1} in DME) 2045 (s), 1999 (vs), 1972 (sh), 1783 (s); ^{13}C NMR (ppm in CD_2Cl_2) 254.6, 203.2, 202.0.

$Co_4(^{13}CO)_9$(tripod). $Co_4(^{13}CO)_9$(tripod) was prepared as described for the unlabeled species employing $Co_4(^{13}CO)_{12}$ (prepared from $Co_4(CO)_{12}$ under an atmosphere of ^{13}CO at 40 °C for 24 h).

(1) Langford, C. H.; Gray, H. B. "Ligand Subsitution Processes"; W. A. Benjamin: New York, 1965.
(2) (a) Basolo, F. *Inorg. Chim. Acta* **1981**, *50*, 65. (b) Angelici, R. J. *Organomet. Chem. Rev.* **1968**, *3*, 173. (c) Dobson, G. R. *Acc. Chem. Res.* **1978**, *9*, 300. (d) Covey, W. D.; Brown, T. L. *Inorg. Chem.* **1973**, *12*, 2820. (e) Darensbourg, D. J. *Adv. Organomet. Chem.* **1982**, *21*, 113.
(3) (a) Malik, S. K.; Poe, A. *Inorg. Chem.* **1978**, *17*, 1484. (b) Bor, G.; Dietler, U. K.; Pino, P.; Poe, A. *J. Organomet. Chem.* **1978**, *154*, 301. (c) Malik, S. K.; Poe, A. *Ibid.* **1979**, *18*, 1241. (d) Darensbourg, D. J.; Baldwin-Zuschke, B. J. *Ibid.* **1981**, *20*, 3846. (e) Sonnenberger, D.; Atwood, J. D. *J. Am. Chem. Soc.* **1982**, *104*, 2113. (f) Darensbourg, D. J.; Baldwin-Zuschke, B. J. *Ibid.* **1982**, *104*, 3906. (g) Atwood, J. D.; Wovkulich, M. J.; Sonnenberger, D. *Acc. Chem. Res.* **1983**, *16*, 350.
(4) Muetterties, E. L.; Burch, R. R., Jr.; Stolzenberg, A. M. *Annu. Rev. Phys. Chem.* **1982**, *33*, 89.
(5) (a) Schmidt, S. P.; Trogler, W. C.; Basolo, F. *Inorg. Chem.* 1982, *21*, 1698. (b) Sonnenberger, D.; Atwood, J. D. *J. Am. Chem. Soc.* **1980**, *102*, 3484. (c) Poe, A. *Inorg. Chem.* **1981**, *20*, 4029, 4032 and references therein. (d) Atwood, J. D. *Ibid.* **1981**, *20*, 4031.
(6) Stolzenberg, A. M.; Muetterties, E. L. *J. Am. Chem. Soc.* **1983**, *105*, 822.
(7) Hepp, A. F.; Wrighton, M. S. *J. Am. Chem. Soc.* **1983**, *105*, 5934.
(8) Coville, N. J.; Stolzenberg, A. M.; Muetterties, E. L. *J. Am. Chem. Soc.* **1983**, *105*, 2499.
(9) Darensbourg, D. J.; Zalewski, D. J., to be submitted for publication.
(10) (a) Arduini, A. A.; Bahsoun, A. A.; Osborn, J. A.; Voelken, C. *Angew. Chem.* **1980**, *92*, 1058; *Angew. Chem., Int. Ed. Engl.* **1980**, *19*, 1024. (b) Osborn, J. A.; Stanley, G. . *Angew. Chem.* **1980**, *92*, 1059; *Angew. Chem., Int. Ed. Engl.* **1980**, *19*, 1025.
(11) Darensbourg, D. J.; Incorvia, M. J. *J. Organomet. Chem.* **1979**, *171*, 89.
(12) Darensbourg, D. J.; Incorvia, M. J. *Inorg. Chem.* **1980**, *19*, 2585.
(13) Darensbourg, D. J.; Incorvia, M. J. *Inorg. Chem.* **1981**, *20*, 1911.
(14) Darensbourg, D. J.; Peterson, B. S.; Schmidt, R. E., Jr. *Organometallics* **1982**, *1*, 306.
(15) Bahsoun, A. A.; Osborn, J. A.; Voelken, C.; Bonnet, J. J.; Lavigne, G. *Organometallics* **1982**, *1*, 1114.

Alternatively $Co_4(^{13}CO)_9$(tripod) was synthesized from $Co_4(CO)_9$(tripod) and ^{13}CO at 60 °C. The infrared spectra of the ^{13}CO-enriched derivatives in the ν(CO) region were identical, i.e., either synthetic route provided the totally enriched sample: IR (cm^{-1} in THF) 1997 (s), 1943 (vs), 1925 (sh), 1743 (s); (cm^{-1} in DME) 1996 (s), 1951 (vs), 1926 (sh), 1741 (s).

(η^6-$CH_3C_6H_5$)$Co_4(CO)_6$(tripod). The π-toluene complex was prepared as previously described.[15]

Kinetic Measurements. The reaction of $Co_4(CO)_9$(tripod) with ^{13}CO was carried out in a 250-mL Schlenk flask. In a typical experiment 0.10 g of $Co_4(CO)_9$(tripod) (0.85 mmol of CO) was dissolved in 10 mL of DME. The solution was then frozen in a dry ice–acetone slush, evacuated, and back-filled with an atmosphere of ^{13}CO (~16 mmol or >18 times excess of ^{13}CO). The reaction flask was then wrapped with aluminum foil to protect the solution from room light and allowed to warm to ambient temperature prior to being placed in a constant temperature bath set at a predetermined temperature. The reaction was followed by intermittently withdrawing samples with a hypodermic syringe and monitoring the infrared spectra in the ν(CO) region. The rate of ^{13}CO incorporation was determined by measuring the disappearance of the peak at 1783 cm^{-1}.

Reactions carried out at pressures greater than atmospheric employed solutions of $Co_4(^{13}CO)_9$(tripod) in DME contained in a thick walled 75-mL Fischer-Porter tube fitted with a pressure gauge and liquid sampling facilities. The apparatus, which was placed inside a plastic shield, was wrapped with aluminum foil to exclude light and equilibrated in a constant temperature water bath prior to introducing 140–170 psi of ^{12}CO. The reaction rate was determined by measuring the disappearance of the peak at 1741 cm^{-1}.

^{13}C NMR Studies. The ^{13}C NMR spectra of $Co_4(CO)_9$(tripod) in CD_2Cl_2 (enriched with 93% and 30% ^{13}CO) were recorded on a Varian XL-200 NMR spectrometer. The spectra were recorded at −80 to 25 °C, and the peak positions were assigned by using the CD_2Cl_2 signal as a reference. The bridging carbonyls gave a signal at 254.7 ppm while the terminal carbonyls gave peaks at 203.2 and 202.0 ppm.

X-ray Experimental Data. A blue parallelepiped shaped crystal measuring 0.5 mm × 0.4 mm × 0.3 mm was sealed in epoxy inside a glass capillary tube in order to prevent atmosphere contact. Intensity data were collected on an Enraf-Nonius CAD4 computer automated diffractometer using Mo Kα radiation (λ = 0.71073 Å). Precise lattice constants determined from 25 well-centered reflections gave the following: a = 21.943 (6) Å, b = 17.289 (7) Å, c = 26.137 (4) Å, α = 90.0°, β = 105.14 (2)°, γ = 90.0°. The cell was indexed as $I2/a$ with Z = 8, body-centered (I) cell was chosen over face-centered (C) for more reasonable β angle (133.9° (C) vs. 105.3° (I)). Unique diffraction data were collected ($h,k \geq 0, \pm l$) in the range $0° < \theta < 22°$. A total of 6104 reflections were collected with 3001 measuring $I > 3\sigma(I)$. Data were corrected for Lorentz and polarization effects but not for absorption (μ = 15.7 cm^{-1}).

Solution and Refinement of the Structure. The locations of the four Co atoms were determined from application of the direct methods portion of the Enraf-Nonius SDP system of programs.[16] Due to the presence of a disordered solvent molecule, refinement was carried out by using the program SHELX '76 for rigid-body calculations.[17] All phenyl rings were refined as rigid bodies by converting approximate coordinates for the six carbon atoms of the ring to a regular hexagon with the C–C bond distance fixed at 1.395 Å. All hydrogen atoms were included in idealized, calculated positions without refinement. The isotropic temperature factors of all phenyl hydrogen atoms were refined as a single, free variable. The disordered tetrahydrofuran solvent molecule was approximated as two rigid five-membered rings of 50% occupancy with one atom of each ring identified as an oxygen atom based solely on trends in temperature factor refinement. All non-phenyl, non-hydrogen atoms of the structure were allowed to refine anisotropically. The structure was refined by using full-matrix weighted least squares with the following functions minimized: $R_1 = \sum||F_o| - |F_c||/\sum|F_o|$ and $R_2 = \{\sum w(|F_o| - |F_c|)^2/\sum|F_o|^2\}^{1/2}$. Model refinement converged at R_1 = 0.052 and R_2 = 0.051 for 324 variables. The largest shift/esd for the final cycle of least squares was 0.6 for one of the disordered O atoms. The largest residual in the final difference Fourier map was less than 0.65 e Å^3 and was located near the disordered solvent molecule. Final positional coordinates are in Table I, bond lengths in Table II (except for those for the rigid bodies that are included in the supplementary material), and representative bond angles in Table III. Anisotropic thermal parameters, hydrogen coordinates and their U values, and structure factor tables are also available as supplementary material.

(16) Sheldrick, G. "SHELX-76, Program for Crystal Structure Determination", 1976.
(17) Enraf-Nonius "Structure Determination Programs" (SDP); Enraf-Nonius: Delft, Holland, 1975 (revised 1981).

Table I. Positional Parameters for $Co_4(CO)_9$(tripod)

atom	x	y	z
Co1	0.43174 (7)	0.22698 (8)	0.19437 (5)
Co2	0.42532 (7)	0.28176 (9)	0.10684 (5)
Co3	0.33811 (7)	0.30165 (9)	0.14878 (6)
Co4	0.35494 (8)	0.16844 (10)	0.11340 (6)
P1	0.47988 (13)	0.32474 (16)	0.24265 (10)
P2	0.47983 (13)	0.38738 (17)	0.13614 (10)
P3	0.36958 (14)	0.41710 (17)	0.18048 (11)
C1	0.4622 (5)	0.1519 (8)	0.2377 (5)
O1	0.4825 (5)	0.1010 (6)	0.2650 (4)
C2	0.4815 (6)	0.2046 (7)	0.1442 (4)
O2	0.5213 (4)	0.1623 (5)	0.1403 (3)
C3	0.3497 (6)	0.2358 (7)	0.2091 (4)
O3	0.3227 (4)	0.2119 (5)	0.2387 (3)
C4	0.3407 (6)	0.3195 (8)	0.0756 (5)
O4	0.3089 (4)	0.3400 (6)	0.0358 (3)
C5	0.4438 (6)	0.2708 (7)	0.0453 (5)
O5	0.4537 (5)	0.2642 (6)	0.0054 (3)
C6	0.3581 (6)	0.0891 (8)	0.1582 (6)
O6	0.3584 (5)	0.0357 (6)	0.1829 (4)
C7	0.3875 (7)	0.1233 (8)	0.0645 (6)
O7	0.4062 (6)	0.0928 (7)	0.0331 (4)
C8	0.2735 (8)	0.1725 (9)	0.0783 (6)
O8	0.2202 (5)	0.1707 (7)	0.0572 (4)
C9	0.2572 (7)	0.3162 (8)	0.1396 (5)
O9	0.2037 (5)	0.3226 (6)	0.1348 (4)
C100	0.4595 (4)	0.4130 (6)	0.1993 (4)

Table II. Selected Bond Distances (Å) for $Co_4(CO)_9$(tripod)

Co1-Co2	2.447 (2)	Co4-C8	1.784 (16)
Co1-Co3	2.456 (2)	P1-C100	1.884 (10)
Co1-Co4	2.546 (2)	P1-C40	1.863 (7)
Co1-P1	2.207 (3)	P1-C50	1.819 (7)
Co1-C1	1.738 (14)	P2-C100	1.873 (9)
Co1-C2	1.952 (13)	P2-C20	1.829 (7)
Co1-C3	1.945 (12)	P2-C10	1.845 (7)
Co2-Co3	2.467 (2)	P3-C100	1.907 (10)
Co2-Co4	2.529 (2)	P3-C30	1.835 (7)
Co2-P2	2.208 (3)	P3-C60	1.834 (8)
Co2-C2	1.904 (13)	C1-O1	1.148 (13)
Co2-C4	1.937 (13)	C2-O2	1.164 (13)
Co2-C5	1.769 (13)	C3-O3	1.166 (12)
Co3-Co4	2.546 (2)	C4-O4	1.146 (13)
Co3-P3	2.203 (3)	C5-O5	1.127 (12)
Co3-C3	1.908 (12)	C6-O6	1.126 (14)
Co3-C4	1.954 (13)	C7-O7	1.140 (14)
Co3-C9	1.748 (16)	C8-O8	1.157 (15)
Co4-C6	1.794 (15)	C9-O9	1.153 (14)
Co4-C7	1.798 (15)		

Results and Discussion

The X-ray Structure of $Co_4(CO)_9$(tripod). Figure 1 presents perspective views of the structure of $Co_4(CO)_9[HC(PPh_2)_3]$ and Figure 2 defines the atomic numbering scheme employed. The molecule contains a central tetrahedron of cobalt atoms symmetrically bridged on three edges by CO groups with the $HC(PPh_2)_3$ ligand capping the CO-bridged triangular face. The structure of the title compound may be discussed in the context of the reported structures of $Co_4(CO)_{12}$,[18] $Co_4(CO)_{11}PPh_3$,[13] $Co_4(CO)_{10}$[P-

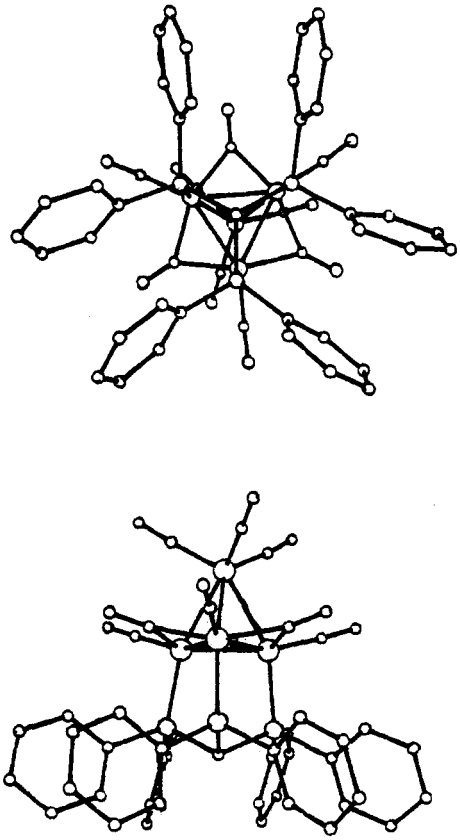

Figure 1. Perspective views of the $Co_4(CO)_9$(tripod) molecule.

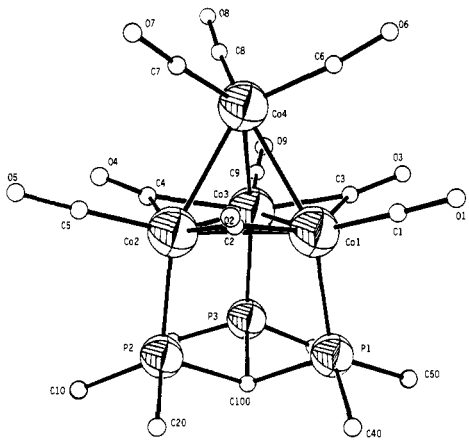

Figure 2. View of the $Co_4(CO)_9$(tripod) molecule giving the atomic numbering scheme. Atoms were assigned arbitrary radii.

$(OMe)_3]_2$,[13] and $(\eta^6\text{-}CH_3C_6H_5)Co_4(CO)_6[HC(PPh_2)_3]$.[15] These comparisons are summarized in Table IV.

A particularly notable finding is the observation that in the three Co_4 carbonyl clusters, containing phosphorus ligands in the basal Co_3 unit and unsubstituted at the apical Co atom, the basal Co–Co bond lengths are all quite similar (2.454–2.482 Å) and significantly shorter than the basal–apical Co–Co bond distances (2.528–2.590 Å). Analogous basal Co–Co bond lengths are exhibited in both (toluene)$Co_4(CO)_6$(tripod) and (π-arene)$Co_4(CO)_9$[19] (π-arene = xylene and benzene) derivatives (2.447–2.455 Å); however, a meaningful shortening of the basal–apical CO

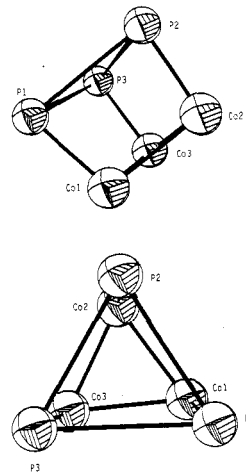

Figure 3. Perspective views of the Co_3P_3 distorted trigonal prism.

bond distances (2.472–2.471 Å) results upon apical substitution by these η^6-arene ligands. Hence, although there is little effect on the Co–Co bond distances upon substitution at the CO-bridged supported Co–Co sites, replacement of the apical CO groups by electron-donating ligands results in a shortening of the basal–apical cobalt bonds. We are currently examining the generality of this observation by investigating the effects of substitution of apical carbon monoxide ligands by phosphorus groups (vide infra). These observations taken together would suggest that Co–Co bonds bridged by CO groups are intrinsically shorter than Co–Co bonds containing no CO bridging ligands.

The two sets of terminal Co–C bond distances display only marginal differences ($<3\sigma$), with the Co–CO apical groups being perhaps a bit longer (0.041 Å). The Co–P bond lengths in both $Co_4(CO)_9$(tripod) and (π-toluene)-$Co_4(CO)_6$(tripod) are slightly shorter than that observed in $Co_4(CO)_{11}PPh_3$ and somewhat longer than those seen in $Co_4(CO)_{10}[P(OMe)_3]_2$, results consistent with alkylphosphine and alkyl phosphite ligands binding to zerovalent metal centers more strongly than aryl phosphines.[20]

The nonbonding P···P distances average 2.992 (4) Å, or about 0.5 Å longer than the average basal Co–Co bond length of 2.457 (2) Å. This is pictorially represented in the skeletal views of the slightly assymmetric trigonal prism formed by the three basal cobalt atoms and the three tripod phosphorus atoms (Figure 3). Although this bite distance might at first glance seem quite correct for the Co_4 unit, where the P–Co–Co (basal) angles average 96.9°,[21] it is a bit short. Instead a P···P distance of 3.8 Å would be more appropriate. That is, in the instances where the axial phosphorus ligands are monoligating as in $Co_4(CO)_{11}PPh_3$ or $Co_4(CO)_{10}[P(OMe)_3]_2$, the average P–Co–Co (basal) bond angles are 115.7° and 111.1°, respectively. Quite similar axial C–Co–Co(basal) bond angles are also observed, i.e., 118.1° and 110.5°, respectively.

Hence, although the match of P···P distances and M–M distances is appropriate in trinuclear clusters where the C(axial)–M–M angles approach 90°, a considerably longer P···P distance is required for maximum P–M orbital overlap in the tetranuclear $M_4(CO)_{12}$ derivatives. The P–C–P angles of the bound tripod ligand average 104.8

(18) (a) Wei, C. H.; Dahl, L. F. *J. Am. Chem. Soc.* **1966**, *88*, 1812. (b) Wei, C. H.; Wilkes, G. R.; Dahl, L. F. *Ibid.* **1967**, *89*, 4792. (c) Wei, C. H. *Inorg. Chem.* **1969**, *8*, 2384. (d) Carre, F. H.; Cotton, F. A.; Frena, B. *Ibid.* **1976**, *15*, 380.

(19) Bird, P. H.; Fraser, A. R. *J. Organomet. Chem.* **1974**, *73*, 103.

(20) (a) Dobson, G. R.; Smith, L. A. H. *Inorg. Chem.* **1970**, *9*, 1001. (b) Wovkulich, M. J.; Atwood, J. D. *J. Organomet. Chem.* **1979**, *184*, 77. (c) Cotton, F. A.; Darensbourg, D. J.; Ilsley, W. H. *Inorg. Chem.* **1981**, *20*, 578.

(21) There is assymetry in the Co_3P_3 trigonal-prismatic unit where each phosphorus atom has two slightly different P–Co–Co(basal) angles averaging 95.4° and 98.4°.

Table III. Selected Bond Angles (deg) for $Co_4(CO)_9$(tripod)

Co3-Co1-Co2	60.4 (1)	Co2-Co3-Co1	59.6 (1)	C100-P2-Co2	105.6 (3)
Co4-Co1-Co2	60.8 (1)	Co4-Co3-Co1	61.2 (1)	C20-P2-Co2	118.8 (2)
Co4-Co1-Co3	61.2 (1)	Co4-Co3-Co2	60.6 (1)	C20-P2-C100	104.6 (4)
P1-Co1-Co2	98.1 (1)	P3-Co3-Co1	98.9 (1)	C10-P2-Co2	118.0 (2)
P1-Co1-Co3	95.1 (1)	P3-Co3-Co2	95.2 (1)	C10-P2-C100	110.1 (4)
P1-Co1-Co4	153.4 (1)	P3-Co3-Co4	153.7 (1)	C10-P2-C20	98.8 (3)
C1-Co1-Co2	144.8 (4)	C3-Co3-Co1	51.1 (4)	C100-P3-Co3	105.4 (3)
C1-Co1-Co3	147.1 (4)	C3-Co3-Co2	109.5 (4)	C30-P3-Co3	119.0 (2)
C1-Co1-Co4	107.7 (4)	C3-Co3-Co4	76.1 (3)	C30-P3-C100	108.1 (4)
C1-Co1-P1	98.8 (4)	C3-Co3-P3	105.6 (4)	C60-P3-Co3	117.3 (2)
C2-Co1-Co2	49.7 (4)	C4-Co3-Co1	108.9 (4)	C60-P3-C100	107.3 (4)
C2-Co1-Co3	108.8 (4)	C4-Co3-Co2	50.4 (4)	C60-P3-C30	99.2 (3)
C2-Co1-Co4	74.2 (3)	C4-Co3-Co4	75.1 (4)	O1-C1-Co1	177.8 (2)
C2-Co1-P1	105.5 (3)	C4-Co3-P3	98.0 (4)	Co2-C2-Co1	78.8 (5)
C2-Co1-C1	95.9 (5)	C4-Co3-C3	150.7 (5)	O2-C2-Co1	138.4 (1)
C3-Co1-Co2	109.0 (3)	C9-Co3-Co1	146.5 (5)	O2-C2-Co2	142.7 (1)
C3-Co1-Co3	49.7 (3)	C9-Co3-Co2	146.9 (4)	Co3-C3-Co1	79.2 (5)
C3-Co1-Co4	75.5 (3)	C9-Co3-Co4	108.6 (5)	O3-C3-Co1	139.5 (1)
C3-Co1-P1	99.0 (3)	C9-Co3-P3	97.4 (5)	O3-C3-Co3	141.2 (1)
C3-Co1-C1	98.5 (5)	C9-Co3-C3	96.3 (6)	Co3-C4-Co2	78.7 (5)
C3-Co1-C2	149.2 (5)	C9-Co3-C4	97.5 (6)	O4-C4-Co2	140.9 (1)
Co3-Co2-Co1	60.0 (1)	Co2-Co4-Co1	57.6 (1)	O4-C4-Co3	140.4 (1)
Co4-Co2-Co1	61.5 (1)	Co3-Co4-Co1	57.7 (1)	O5-C5-Co2	177.9 (2)
Co4-Co2-Co3	61.3 (1)	Co3-Co4-Co2	58.2 (1)	O6-C6-Co4	174.5 (2)
P2-Co2-Co1	95.9 (1)	C6-Co4-Co1	81.8 (4)	O7-C7-Co4	177.4 (3)
P2-Co2-Co3	98.2 (1)	C6-Co4-Co2	135.8 (4)	O8-C8-Co4	175.5 (5)
P2-Co2-Co4	154.5 (1)	C6-Co4-Co3	116.1 (4)	O9-C9-Co3	176.8 (3)
C2-Co2-Co1	51.5 (4)	C7-Co4-Co1	117.7 (5)	P2-C100-P1	105.4 (5)
C2-Co2-Co3	110.1 (4)	C7-Co4-Co2	85.7 (4)	P3-C100-P1	104.6 (5)
C2-Co2-Co4	75.4 (3)	C7-Co4-Co3	140.7 (4)	P3-C100-P2	104.5 (5)
C2-Co2-P2	100.5 (3)	C7-Co4-C6	100.2 (6)	C21-C20-P2	122.0 (2)
C4-Co2-Co1	109.8 (4)	C8-Co4-Co1	140.2 (5)	C25-C20-P2	117.4 (2)
C4-Co2-Co3	51.0 (4)	C8-Co4-Co2	118.8 (5)	C11-C10-P2	121.6 (2)
C4-Co2-Co4	75.8 (4)	C8-Co4-Co3	86.0 (5)	C15-C10-P2	118.4 (2)
C4-Co2-P2	103.9 (4)	C8-Co4-C6	103.2 (6)	C31-C30-P3	118.1 (2)
C4-Co2-C2	150.9 (5)	C8-Co4-C7	100.5 (7)	C35-C30-P3	121.8 (2)
C5-Co2-Co1	147.0 (4)	C100-P1-Co1	105.9 (3)	C41-C40-P1	121.7 (2)
C5-Co2-Co3	144.0 (4)	C40-P1-Co1	116.7 (2)	C45-C40-P1	118.2 (2)
C5-Co2-Co4	105.6 (4)	C40-P1-C100	110.8 (4)	C51-C50-P1	118.3 (2)
C5-Co2-P2	99.9 (4)	C50-P1-Co1	118.6 (2)	C55-C50-P1	118.8 (2)
C5-Co2-C2	96.9 (5)	C50-P1-C100	105.6 (4)	C61-C60-P3	122.0 (2)
C5-Co2-C4	94.3 (5)	C50-P1-C40	98.8 (3)	C65-C60-P3	117.5 (2)

(5)°, which is not exceptional. Thus there is angle strain in the Co–P bonds in $Co_4(CO)_9$(tripod). This might be compensated for somewhat with a larger capping atom for the three phosphorus ligating sites, e.g., silicon as in $MeSi(PBu_2)_3$.[22] It would further be anticipated that this angle strain in the M–P bond would increase upon proceeding down the group 8B metal series.

Ligand Substitution Processes in $Co_4(CO)_9$(tripod). Carbon monoxide exchange reactions of $Co_4(CO)_9$(tripod) employing ^{13}CO as incoming ligand were measured at several temperatures in dimethoxyethane. Table V contains rate data for CO displacement from the Co_4 unit as a function of both temperature and carbon monoxide pressure. Rate constants were determined at atmospheric CO pressure by monitoring the decrease in absorptions in the bridging ν(CO) region due to the all ^{12}CO species as described in our previous publications (Figure 4).[11-14] The incoming ^{13}CO ligands were statistically distributed throughout the cluster under the conditions of ligand substitution as evidenced by ^{13}C NMR, where the spectrum for the $Co_4(CO)_9$(tripod) species derived from $Co_4(^{13}CO)_{12}$/tripod and ^{13}CO incorporation into $Co_4(CO)_9$(tripod) were identical (Figure 5). A similar conclusion was reached by Osborn et al. for the ^{13}CO reaction with $Rh_4(CO)_9$(tripod).[15] Hence, intramolecular CO migration over the cluster surface, albeit slow as evidenced by ^{13}C NMR, occurs more rapidly than intermolecular CO ex-

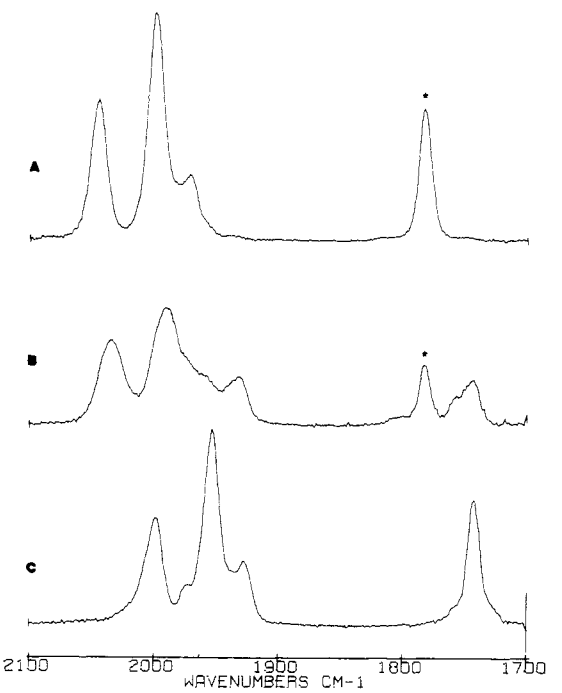

Figure 4. Infrared spectra in the ν(CO) stretching region of $Co_4(CO)_9$(tripod) during the incorporation of ^{13}CO (peak marked by asterisk used in monitoring decrease in $Co_4(CO)_9$(tripod) concentration with time): A, initial $Co_4(^{12}CO)_9$(tripod); B, $Co_4(CO)_9$(tripod) after considerable ^{13}CO incorporation; C, final $Co_4(^{13}CO)_9$(tripod).

(22) De Boer, J. J.; Van Doorn, J. A.; Masters, C. *J. Chem. Soc., Chem. Commun.* **1978**, 1005.

Table IV. Comparative Bond Distances (Å) in $Co_4(CO)_{12-n}L_n$ Derivatives

bond type	$Co_4(CO)_9$(tripod)		(π-toluene)$Co_4(CO)_6$(tripod)[15]		$Co_4(CO)_{12}$[18]		$Co_4(CO)_{11}[P(C_6H_5)_3]$[13]		$Co_4(CO)_{10}[P(OCH_3)_3]_2$[13]	
	av	range	av	range	av	range	av	range	av	range
Co–Co										
basal-apical	2.540	2.529–2.546	2.472	2.448–2.490	2.492	2.457–2.527	2.530	2.523–2.542	2.528	2.518–2.538
basal-basal	2.457	2.447–2.467	2.447	2.438–2.456			2.482	2.468–2.491	2.454	2.447–2.464
Co–C(br)	1.933	1.904–1.954	1.912	1.89–1.94	2.043	1.958–2.191	1.937	1.887–1.976	1.929	1.879–1.972
Co–C(term)										
apical	1.793	1.784–1.798					1.827	1.822–1.832	1.810	1.797–1.817
equatorial	1.752	1.738–1.769	1.753	1.74–1.77	1.834	1.610–2.032	1.771	1.758–1.778	1.757	1.746–1.775
axial							1.792	1.789–1.794	1.787	1.787
	(1.773)[a]		(1.753)[a]		(1.834)[a]		(1.797)[a]		(1.784)[a]	
Co–P	2.206	2.203–2.208	2.188	2.174–2.202			2.246		2.158	2.156–2.159

[a] The value in parentheses corresponds to the average terminal Co–C distance.

Table V. Temperature Dependence of the Rate of Reaction of $Co_4(CO)_9$(tripod) + ^{13}CO and $Co_4(^{13}CO)_9$(tripod) + CO

temp, °C	10^4k,[a] s^{-1}	temp, °C	10^4k,[a] s^{-1}
	$Co_4(CO)_9$(tripod) + ^{13}CO		
49.40	6.53 ± 0.11	58.00	14.20 ± 0.84
50.60	6.42 ± 0.24	64.15	28.90 ± 1.10
51.75	7.52 ± 0.12	68.10	45.20 ± 2.60
53.51	7.70 ± 0.10		
	$Co_4(^{13}CO)_9$(tripod) + CO (160 psi)		
50.40	5.3 ± 0.8	61.65	17.2 ± 2.0
57.50	10.6 ± 1.7	65.50	44.1 ± 4.8

[a] The rate of reaction is $^7/_3k_{obsd}$, since there are seven positions for a single incoming labeled carbon monoxide ligand to distribute itself among to afford one bridging labeled carbon monoxide group and there is selective dissociation of one of the three equivalent apical CO groups. Error limits represent 90% confidence level.

change. It is this feature of these reactions coupled with the lack of mixing of terminal and bridging CO stretching modes that allows for convenient, quantitative monitoring of the intermolecular CO exchange processes as described above.

The three carbon resonances assignable to CO ligands in the ^{13}C NMR spectrum of $Co_4(CO)_9$(tripod) at 254.6, 203.2, and 202.0 ppm in CD_2Cl_2 (Figure 5) are interpreted as being due to bridging, apical, and equatorial CO groups, respectively. The apical assignment for the resonance at 203.2 ppm is based on the temperature dependence of this peak, where a rapid intramolecular exchange of these carbonyl groups occur about the C_3 axis at ambient temperature. This feature is as well seen in both ^{13}C and ^{31}P NMR spectra of $P(OMe)_3$ and PMe_3 apically substituted $Co_4(CO)_9$(tripod) derivatives,[23] where the signals for the apical CO and phosphorus ligands are only observed at low temperature.

For an investigation of the effect of carbon monoxide pressure on the rate of CO ligand exchange, samples of $Co_4(CO)_9$(tripod) completely enriched in ^{13}CO were allowed to undergo reaction with ^{12}CO, i.e., the reverse of the process employed for atmospheric carbon monoxide pressure (eq 5). This procedure is used to make more efficient use of the expensive ^{13}C isotopically labeled substrate.

$$Co_4(^{13}CO)_9(\text{tripod}) + n^{12}CO \rightleftharpoons Co_4(^{13}CO)_{9-n}(^{12}CO)_n(\text{tripod}) + n^{13}CO \quad (5)$$

A CO dissociative reaction pathway would not be expected to display a dependence on the concentration of the incoming ligand. However, if metal–metal bond fission with subsequent addition of the entering ^{13}CO ligand at the site of unsaturation is rate limiting, an increase in reaction rate with increasing CO pressure would be anticipated. Activation parameters derived from rate constants with or without inclusion of the higher pressure data were approximately the same, thus indicating a lack of sensitivity of the rate to the incoming CO ligand concentration. Concomitant with this observation the activation parameters are consistent with a CO dissociative process. On the other hand, reactions involving PMe_3 and $P(OMe)_3$ as entering ligands lead to rapid formation of a monosubstituted species (much faster than the ^{13}CO substitution process), followed by slower processes that result in higher

(23) Work is presently underway in our laboratories to more fully characterize these substituted $Co_4(CO)_9$(tripod) derivatives by IR and NMR spectroscopy and X-ray crystallography.

Table VI. Comparative Rates and Activation Parameters for Carbon Monoxide Displacement in $Co_4(CO)_{12}$ Derivatives

complex	10^4k,[a] s^{-1}	ΔS^*,[b] kcal mol^{-1}	ΔS^*,[b] eu
$Co_4(CO)_{12}$	3.27 (1.91)	24.9 ± 1.9	2.9 ± 5.9
$Co_4(CO)_{11}P(OMe)_3$	2.03 (1.19)	26.8 ± 1.0	8.2 ± 3.5
$Co_4(CO)_{11}P(OEt)_3$	3.37 (1.97)	27.5 ± 3.3	11.0 ± 10.2
$Co_4(CO)_{11}PEt_3$	15.60 (9.12)		
$Co_4(CO)_{10}[P(OMe)_3]_2$	4.77 (2.79)	27.1 ± 1.1	10.7 ± 3.7
$Co_4(CO)_9$(tripod)[c]	1.71 (1)	24.2 ± 3.3	−0.52 ± 10.2

[a] For the reaction $Co_4(CO)_{12-n}L_n$ + (excess)$^{13}CO \rightarrow Co_4(^{13}CO)_{12-n}L_n + {}^{12}CO$ at 40 °C; values in parentheses represent relative rates. [b] Error limits represent 90% confidence limits. [c] Derived from both low- and high-pressure data. With use of atmospheric pressure data only values of $\Delta H^* = 23.1 \pm 2.4$ kcal mol^{-1} and $\Delta S^* = -3.98 \pm 7.4$ eu were obtained.

degrees of CO replacement. This occurrence is congruous with the much greater nucleophilicity of phosphorus donor ligands as compared with carbon monoxide and has also been seen for substitution into the parent $Co_4(CO)_{12}$ species.[11-14]

The rate constants listed in Table V were computed by assuming the stereoselective dissociation of three carbon monoxide ligands in $Co_4(CO)_9$(tripod). These are assumed to be the three apical carbonyl groups based on the following rationale. Crystal structure data suggest that of the two different terminal carbon monoxide binding sites, the apical groups are slightly weaker bonded. Second, substitution reactions of $Co_4(CO)_9$(tripod) with phosphorus ligands results ostensibly in apical CO displacement. Third, when there are no apical carbon monoxide ligands as in (toluene)$Co_4(CO)_6$(tripod), no carbon monoxide intermolecular exchange reactions are observed even at temperatures up to 160 °C in decane. In addition, Osborn and co-workers[15] have reported that the apical CO groups in $Ir_4(CO)_9$[tripod] appear to undergo preferential intermolecular carbon monoxide exchange with ^{13}CO.

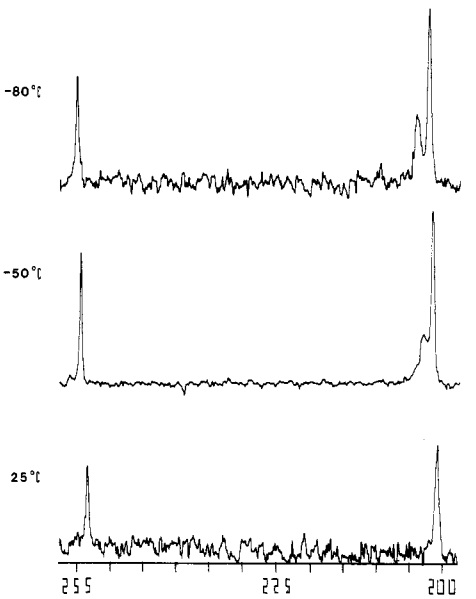

Figure 5. Temperature-dependent ^{13}C NMR spectra of $Co_4(CO)_9$(tripod) in CD_2Cl_2 solvent.

Conclusions

Summarized in Table VI are the comparative specific rate constants and activation parameters for CO ligand substitutional processes in the tetranuclear cobalt carbonyl cluster and its derivatives containing phosphorus ligands. Our most recent efforts on the $Co_4(CO)_9$(tripod) derivative further corroborate the previously observed lack of sensitivity of phosphorus ligand substitution on the rate of CO displacement from the Co_4 unit. Namely, rate changes for CO substitution as a function of prior substitution at the metal centers in $Co_4(CO)_{12}$ by phosphorus ligands occupying axial coordination sites are minimal (eq 6). Less

$$Co_4(CO)_{12} \xrightarrow[+L]{-CO} Co_4(CO)_{11}L \xrightarrow[+L]{-CO} Co_4(CO)_{10}L_2 \xrightarrow[+L]{-CO} Co_4(CO)_9L_3 \xrightarrow[+L]{-CO} Co_4(CO)_8L_4 \quad (6)$$

than an order of magnitude separates the spread in rate constants for CO dissociation in all the complexes examined to date. When the sterically more demanding PEt_3 ligand is excluded, these rate constants differ by less than a factor of 3. On the other hand replacement of the three apical CO groups in $Co_4(CO)_9L_3$ by π-arene ligands, where all the metal centers bear electron donor ligands, greatly retards the rate of further CO dissociation.

It should be pointed out that this interpretation is not prejudiced by the assumption made with regard to the number of dissociable CO groups in the various Co_4 clusters. The relative order of reactivity as provided in Table VI is based on stereoselective dissociation of the three axial CO groups in $Co_4(CO)_{12}$, two axial CO groups in $Co_4(CO)_{11}L$ (L = $P(OMe)_3$, $P(OEt)_3$, PEt_3), one axial CO group in $Co_4(CO)_{10}[P(OMe)_3]_2$, and three apical CO groups in $Co_4(CO)_9$(tripod). Alternatively, quite similar relative rate constants for CO dissociation are derived on the basis of stereoselective dissociation of three apical CO groups in all cases or by assuming all CO groups are equally dissociable.[24]

The more significant contribution of this present investigation is that the carbon monoxide substitutional parameters for the highly constrained $Co_4(CO)_9$(tripod) species are very much like those of the parent $Co_4(CO)_{12}$ species and its monoligated phosphorus ligand derivatives. This is strongly suggestive of a common mechanistic pathway operating for all of these intermolecular CO exchange processes. It has further been demonstrated that $Co_4(CO)_9$(tripod) in the presence of carbon monoxide does not fragment even under forcing conditions (100 °C and 30 bar pressure)[15] and that cluster fragmentation is not important in substitution reactions of $Co_4(CO)_{12}$ with $P(OMe)_3$.[9] Therefore we would conclude that intermolecular carbon monoxide exchange reactions in the $Co_4(CO)_{12}$ derivative thus far studied are taking place via a simple CO dissociative (D) process. Presumably an analogous reaction pathway would maintain for the remaining members of the group 8B metals (Rh and Ir), where stronger metal–metal bonds exist.[3d,f,25] It is however to be expected that in CO displacement reactions by phosphine, phosphite, and other donor ligands more complicated reaction pathways are likely to be operative. These processes are avoided by the methodology centered around the utiliza-

(24) The computed relative rates for CO dissociation employing these two models are 2.42:1.00:1.67:7.70:1.18:1.27 and 2.20:1.00:1.67:7.70:1.29:1.54, respectively.

(25) Substitutional processes involving the $Rh_4(CO)_9$(tripod) derivative are being investigated mechanistically in the laboratory of Professor F. Basolo (Northwestern University).

tion of ^{13}CO as the incoming ligand.

Acknowledgment. The financial support of the Robert A. Welch Foundation is greatly appreciated. We are also grateful to Professors J. A. Osborn and G. G. Stanley for supplying important experimental details prior to publication.

Registry No. $Co_4(CO)_9$(tripod), 75801-99-9; $Co_4(^{13}CO)_9$(tripod), 89958-44-1; $(\eta^6\text{-}CH_3C_6H_5)Co_4(CO)_6$(tripod), 82264-80-0; ^{13}CO, 1641-69-6; CO, 630-08-0.

Supplementary Material Available: Tables of coordinates and isotropic thermal parameters for phenyl rings in $Co_4(CO)_9$(tripod) and anisotropic thermal parameters, hydrogen coordinates, and structure factor amplitudes for $Co_4(CO)_9$(tripod) (21 pages). Ordering information is given on any current masthead page.

Reactions of WCl_2L_4 (L = a Phosphine). 1.[1] A New Class of Tungsten(II) Ethylene Complexes

Paul R. Sharp

Department of Chemistry, University of Missouri—Columbia, Columbia, Missouri 65211

Received January 23, 1984

WCl_2L_4 can be prepared by reducing WCl_4L_n with 2 equiv of sodium amalgam in the presence of L (L = PMe_3, n = 3; L = PMe_2Ph and $PMePh_2$, n = 2). Phosphine is displaced from WCl_2L_4 by ethylene to give first $WCl_2L_3(C_2H_4)$ (L = PMe_3) and then $WCl_2L_2(C_2H_4)_2$. $WCl_2(PMe_3)_2(C_2H_4)_2$ reacts with $TlBF_4$, $AlCl_3$, and $AlMe_3$ to give cationic complexes. The X-ray crystal structure of one of these, $[WMe(PMe_3)_2(C_2H_4)_2][ClAlMe_xCl_{3-x}]$, was determined. The crystals are monoclinic ($P2_1/n$) with a = 9.922 (2) Å, b = 7.419 (1) Å, c = 29.241 (4) Å, β = 92.79 (2)°, V = 2150 Å^3, and Z = 4. The three-dimensional X-ray data were measured with the θ–2θ scan technique with a scintillation detector. The structure was resolved by Patterson and Fourier methods and refined by full-matrix least-squares calculations to give $R(F_o)$ = 0.025 and $R_w(F_o)$ = 0.032 for 1362 observations above 2σ. The solid state structure consists of monomeric units with cis ethylenes, trans phosphines, and a weakly coordinated aluminate. NMR and conductivity data suggest the equilibrium in solution of this structure with an ionic complex formed by loss of the aluminate. The reaction of this complex with tmeda (*N,N,N',N'*-tetramethylethylenediamine) or other Lewis bases gives neutral $WMeCl(PMe_3)_2(C_2H_4)_2$ that loses Cl^- in polar, noncoordinating solvents.

Introduction

We recently communicated the preparation of $WCl_2(PMe_3)_4$ (**1a**) and its use to prepare tungsten methylidyne complexes[2] and a complex containing a W–W quadruple bond.[3] We now wish to report the full details of the preparation of WCl_2L_4 (L = PMe_3, PMe_2Ph, and $PMePh_2$) and reactions of these versatile starting materials with ethylene. The ethylene products and their derivatives comprise a new class of tungsten(II) ethylene complexes that, in a broader sense, are members of a group of W(II) and Mo(II) complexes which contain both π-acids and π-bases in their coordination sphere.

Such complexes have recently attracted attention from both a synthetic[4] and a theoretical[5] point of view. Many members of this group are considered unusual in that their formal electron count is only 16 yet they show low electrophilicity. This observation has been attributed to stabilization by π-donation from the π-base ligands.[4] The new members reported here also follow this pattern but in addition show a tendency to further decrease their electron count by the loss of ethylene, phosphine, or Cl^-. In one case the loss of Cl^- gives a stable, formally 14-electron complex with no π-base ligands in its coordination sphere.

Results

Reduction of WCl_4L_n. Treating $WCl_4(PMe_3)_3$ with 2 equiv of sodium amalgam (0.4%) in the presence of PMe_3 gives high yields of $WCl_2(PMe_3)_4$ (**1a**, eq 1). Although **1a**

$$WCl_4(PMe_3)_3 + 2Na/Hg \xrightarrow[THF]{PMe_3} \underset{\mathbf{1a}}{WCl_2(PMe_3)_4} \quad (1)$$

is paramagnetic (μ_{eff} = 2.3 μ_B), a single, broad resonance is observed in its ^1H NMR spectrum at 3.8 ppm, suggesting that the chlorides in **1a** are trans. Analogous complexes can be prepared with other phosphines by reducing WCl_4L_2 (L = PMe_2Ph and $PMePh_2$) in the presence of L, but the yields are lower and the products are harder to isolate.

A related complex, $WCl_2(bpy)(PMe_3)_2$, results when $WCl_4(bpy)$ is reduced in the presence of PMe_3 (eq 2). The

$$WCl_4(bpy) + 2Na/Hg + 2PMe_3 \rightarrow WCl_2(bpy)(PMe_3)_2 \quad (2)$$

^1H NMR of this complex indicates that it too is paramagnetic. The ^1H NMR of this complex indicates that it too is paramagnetic. No signal for the bpy ligand could be detected, and the signal for the PMe_3 protons is found at −6 ppm. The fact that this signal is a virtual triplet

(1) Part 2 deals with hydride complexes derived from the addition of H_2 to $WCl_2(PMe_3)_4$. Frank, K. G.; Sharp, P. R., to be submitted for publication in *Inorg. Chem.*

(2) Sharp, P. R.; Holmes, S. J.; Schrock, R. R.; Churchill, M. R.; Wasserman, H. J. *J. Am. Chem. Soc.* **1981**, *103*, 965. Churchill, M. R.; Rheingold, A. L.; Wasserman, H. J. *Inorg. Chem.* **1981**, *20*, 3392.

(3) (a) Sharp, P. R.; Schrock, R. R. *J. Am. Chem. Soc.* **1980**, *102*, 1430. (b) Schrock, R. R.; Sturgeoff, L. G.; Sharp, P. R. *Inorg. Chem.* **1983**, *22*, 2801.

(4) Herrich, R. S.; Nieter-Burgmayer, S. J.; Templeton, J. L. *J. Am. Chem. Soc.* **1983**, *105*, 2599 and references cited therein.

(5) Kubacek, P.; Hoffmann, R. J. *J. Am. Chem. Soc.* **1981**, *103*, 4320.

0276-7333/84/2303-1217$01.50/0